Available online at www.sciencedirect.com
ScienceDirect
Journal of Sound and Vibration 298 (2006) 688–703
JOURNAL OF SOUND AND VIBRATION
www.elsevier.com/locate/jsvi

Preliminary results on an x-direction apparent mass model of human body sitting in a cushioned, suspended seat

George Juraj Stein*, Peter Múčka, Rudolf Chmúrny

Institute of Materials and Machine Mechanics, Slovak Academy of Sciences, Račianska 75, SK-831 02 Bratislava 3, Slovak Republic

Received 2 May 2006; received in revised form 11 May 2006; accepted 8 June 2006
Available online 14 August 2006

Abstract

For modelling purposes and for evaluation of driver's seat performance in the vertical direction various mechano-mathematical models of seated human body have been developed and standardised by the international organisation for standardisation. No such models currently exist for human body sitting in an upright or slightly inclined position in a cushioned "armchair" type seat upper part, mounted on a mechanical, pneumatic or other type vertical suspension system. The interaction with the steering wheel and/or pedals has to be taken into consideration, as well as the variable position of the upper part of the human body in respect to the cushioned back-support of a driver's seat (full back contact to no contact at all), as observed in real driving conditions. This complex problem has to be simplified first to arrive at a manageable simpler mechano-mathematical model which still reflects the main problem features.

A simple linear model of the human body apparent mass in the x-direction was designed and analysed. The model accounts for the reaction from the steering wheel and contact with the cushioned back-support of the seat "armchair" part. Model parameters were identified on basis of laboratory measurements. Out of three possible variant the most appropriate was singled out. The proposed model describes the measured apparent mass curve, and also gives indicative prediction of vibration transmissibility across the fore-and-aft (x-direction) suspension system, if mounted and enabled. The proposed model can be a starting point for a further research in this field.

1. Introduction

The biodynamic response of human body to vibration and shocks is a vastly complex problem, which has been of considerable interest for decades. A comprehensive description of all the aspects of the problem can be found e.g. in Refs. [1–3]. Exposure to excessive vibration causes discomfort and hampers handling of vehicles and mobile machinery. Prolonged exposure may cause permanent changes in the health condition and even to irreversible deterioration of health, leading in exceptional cases to permanent work disability. Hence, preventive measures have to be taken by suitable technical means to minimise the adverse influence of vibration on the human body. One of the persistent problems in human body dynamic response modelling is the design of a faithful but reasonably simple model of the human body in various positions occurring in

*Corresponding author. Tel.: +4212 5930 9422; fax: +4212 5477 2909.
E-mail address: stein@savba.sk (G.J. Stein).

0022-460X/$ - see front matter © 2006 Elsevier Ltd. All rights reserved.
doi:10.1016/j.jsv.2006.06.009

practice, e.g. sitting in a suspended cushioned driver's seat. A lot of work on this issue has been done for the vertical (z-axis) direction, e.g. [1,4,5]. In the fore-and-aft and lateral directions, however, not many results have been published. Probably, the most comprehensive human body response measurements in the for-and-aft direction (x-axis) and in the lateral direction (y-axis) have been reported in Refs. [6–8] and recently by Fleury [9]. The papers [6–8] are concerned with measurement of human body sitting upright on a rigid seat in a well-defined biodynamical position without interaction with controls. This approach is well justified for biodynamical research purposes, however does not bring full answers to some practical problems. Driven by practical problems, also in view of the EC Directive 2002/44/EC, a pan-European project dealing also with analysis and mitigation of fore-and-aft, as well as, lateral vibrations, with acronym "VIBSEAT" (Project Code G3RD-CT-2002-00827) has been initiated. One specific problem of the many various problems considered within this project was the development of a simple human body model accounting for:

- interaction with vehicle controls and resulting force reactions,
- influence of sitting posture,
- influence of cushioned seat in contrary to a hard support,
- influence of horizontal seat suspension system on vibration mitigation.

Various approaches to human body modelling can be found in the relevant literature, mainly for the vertical direction. There are no reliable models for the fore-and-aft direction. Hence, an attempt has been made to develop simple human body models from linear translatory "building elements"—masses, linear springs and viscous dampers to arrive at reasonable simple, yet faithful representations, which are justified form physical and biodynamical point of view. Other approaches are feasible, e.g. using also rotational "building elements", as reported by another project partner [10]. The models were partially validated in respect to laboratory measurements with a single person on a seat with horizontal seat suspension system, as supplied by one of the project partners.

2. Aims of the paper

2.1. Human body apparent mass in the vertical direction

Human body apparent mass and/or driving point mechanical impedance in the vertical direction is a well-established descriptor in bio-dynamics and in research of human influence of vibrations [1,4,5]. Furthermore, the international standardisation in this field is well advanced within the ISO TC 108/SC5 and CEN TC 231 Committees. The results of this standardisation are two current standards [11,12], amalgamating most of the hitherto reported laboratory measurements.

The basic definitions of human body driving point mechanical impedance $\mathbf{Z}(\omega)$ and of the apparent mass in vertical direction $\mathbf{M}(\omega)$ as a function of angular frequency $\omega = 2\pi f$ from a given frequency range are following:

(A) *The driving point mechanical impedance* $\mathbf{Z}(\omega)$: is the complex ratio of an applied periodic excitation of a system (force $\mathbf{F}(\omega)$) to its response (velocity $\mathbf{v}(\omega)$), measured in the same point and same direction as the applied force:

$$\mathbf{Z}(\omega) = \frac{\mathbf{F}(\omega)}{\mathbf{v}(\omega)}. \tag{1}$$

(B) *The apparent mass* $\mathbf{M}(\omega)$: is the complex ratio of an applied periodic excitation of a system (force $\mathbf{F}(\omega)$) to its response (acceleration $\mathbf{a}(\omega)$) in the same point and the same direction, both being complex quantities:

$$\mathbf{M}(\omega) = \frac{\mathbf{F}(\omega)}{\mathbf{a}(\omega)}. \tag{2}$$

Both apparent mass and mechanical impedance are complex functions of the real argument ω; the angular frequency $\omega = 2\pi f$, where f is frequency in Hz.

2.2. Aims of the research

Various further approaches to modelling of seated human body are used [1,13,14] to quote but a few, however no information is available on modelling of the seated human body behaviour in the fore-and-aft (x-axis) direction. Hence, the aim of this research is to propose a simple model of seated human body in the horizontal (x-axis) direction and validate it to available measured data with the aim to use this model further in driver's seat horizontal (x-axis) vibration isolation system (VIS) modelling. In defining these aims a suitable model must fulfil following requirements:

(i) Faithfully represent the apparent mass while the seat horizontal VIS is blocked or enabled,
(ii) Enable to assess the acceleration transmissibility through the horizontal VIS.

The first requirement means that the model has to describe the experimentally measured apparent mass data faithfully, while the second requirement means that the model has to be applicable for reasonable predictions of the seat horizontal VIS performance. The fore-and-aft VIS loaded by the identified apparent mass model has to exhibit essentially the same acceleration transmissibility T_x course as measured in laboratory otherwise the model would not be usable for seat suspension system performance prediction. In this capacity, the dual-purpose model would be usable in seat research, as well as, present a good mechano-mathematical representation of the measured data. Moreover, the model has to be reasonably simple. Future research employing a larger set of experimental data may refine this model.

3. Seat back contact considerations

The driver can take different positions in the seat's cushioned armchair, which may be representative of various classes of machines:

(i) The driver/operator is firmly belted to the seat back by a multipoint seat belt. This position would possibly correspond to driver/passenger in a passenger car, albeit in this situation the back angle would exceed the stipulated 10° [14].
(ii) The driver/operator/passenger would sit comfortably in the seat, hands in lap (HIL) or loosely on controls. A full contact with the seat back would be maintained at all instants. This would correspond to operator's position without using a steering wheel, or a position of a seated rail passenger or a long-distance bus passenger. This corresponds to situation 4 in Fig. 1.

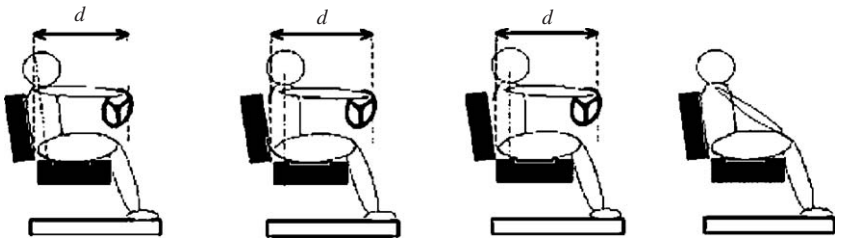

Fig. 1. Different measuring situations (human body positions in respect to seat backrest).

(iii) The driver/operator often changes position in the seat. The upper contact at the shoulder blades is intermittent, however a full contact at the lower back is maintained in all situations. Such a situation may arise in earth moving machines and construction equipment, as well as in rail engines.
(iv) The driver/operator has his feet on pedals and hands on the steering wheel (position hands on wheel—HOW). The distance from the steering wheel is fixed and depends on ergonomic position of the driver. The upper part of the human body may have firm full contact with the seat back at the shoulder blades (situation 1) in Fig. 1, or only contact in the lumbar region (situation 2) in Fig. 1, or no contact with the back at all (situation 3). The back contact and distance to the steering wheel would markedly influence the system dynamic properties and hence the measured apparent mass.
(v) The driver/operator has his feet on stipulated pedals and hands on steering wheel, however he is sitting on a rigid metallic seat plate, approximately corresponding to the seat frame, with back contact.
(vi) The driver/operator has his feet on stipulated pedals and HIL, however he is sitting on a rigid metallic seat without any back contact. This is the stipulated measuring position HOW for standard biodynamic measurements, for example used in Ref. [1].

All these different positions manifest in measured apparent mass curves. For illustration in Fig. 2 measured apparent mass moduli are depicted as a function of distance d between the stipulated wheel and the seat. For comparison also the measurements, reported in Ref. [1] are included. Note the height of the peak for different distances d, at approximately the same damped natural frequency f_0, as well as, same peak height for both HIL measurements, taken by two different authors in different conditions.

4. Development of the model structure

4.1. Basic assumptions

Prior to the development of a seated human body model in interaction with a cushioned suspended seat and controls some preliminary assumptions have to be made:

(A) The vertical direction vibrations will not be analysed at all.
(B) The possible pitch influence will be neglected. It will be assumed that only horizontal fore-and-aft vibrations are excited.

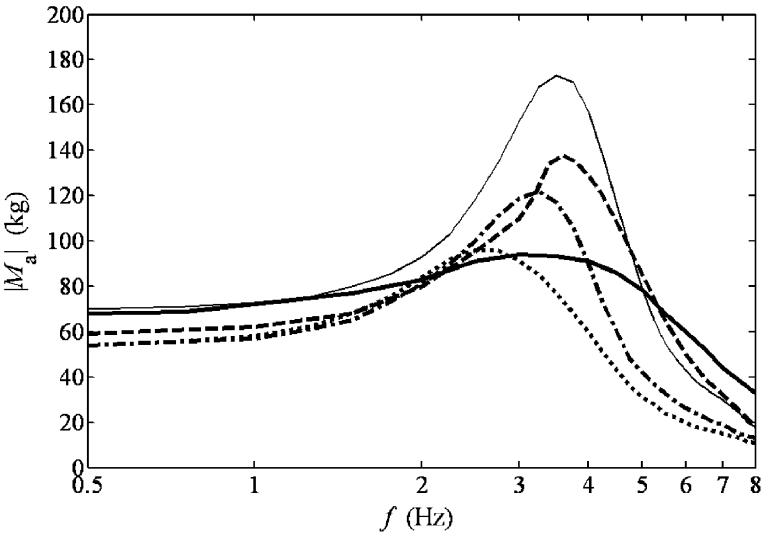

Fig. 2. Moduli of apparent mass as measured for different distances d by Fleury [9]: $d = 100/150$ mm (——), $d = 200/250$ mm (▬ ▬ ▬), $d = 300$ mm (▬ ● ▬), HIL (● ● ●) and for HIL by [6] (▬).

(C) The seat components will be assumed to be sufficiently rigid not to take into consideration any torsion movements, e.g. of the armchair frame. Also, possible resonance due to "armchair" seat part structural elements oscillations will not be taken into account.

(D) No separate consideration of the human body and the seat with its cushioning will be attempted at this stage. The data currently available do not give sufficient information for the decomposition. Hence, the whole complex of seated human body and the "armchair" part of the driver's seat will be considered as single entity. Interaction with the pedals is neglected at this stage; interaction with the steering wheel, however, is included.

(E) No separate consideration of the soft cushioned back-support, embedded in a rigid seat frame, and the human body back is attempted at this stage. Thus, the soft tissues of the human body in contact with the respective cushions and the respective cushions are considered as a single structural element.

(F) The human body, together with the assumed reactions will be taken as a lumped parameters multibody linear model, without going into detailed description of various human body segments and their respective interactions.

4.2. A simple sdof model of the x-direction apparent mass

The apparent mass modules curves shown in Fig. 2 indicate that sdof-like structure of the model with the distance d being a parameter, influencing the assumed linear stiffness coefficient k_1 and linear damping coefficient c_1, could be an appropriate model, as depicted in Fig. 3.

The variables used are:

m_1… base mass, stipulated to be $m_1 = 5.0\,\text{kg}$,
m_2… oscillating mass, probably dependant on the seated human body mass,
k_1… stipulated stiffness, accounting for all elastic interactions,
c_1… coefficient of linear viscous damping, accounting for all vibratory power dissipating mechanisms in the system.

The driving point mechanical impedance of the seated human body in the fore-and-aft direction $\mathbf{Z}_x(\omega)$, in an analogy to a simple model of apparent mass described in Ref. [12], represented by the sdof model of Fig. 3 is

$$\mathbf{Z}_x(\omega) = j\omega m_1 + \frac{\left(\frac{k_1}{j\omega} + c_1\right) j\omega m_2}{\frac{k_1}{j\omega} + c_1 + j\omega m_2}. \tag{3}$$

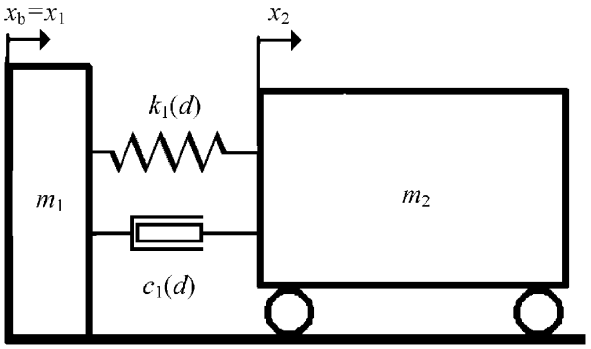

Fig. 3. A single dof apparent mass model structure.

The apparent mass of the seated human body in the for-and-aft direction $\mathbf{M}_x(\omega)$ is, according to Eq. (2) for this case:

$$\mathbf{M}_x(\omega) = m_1 + \frac{(k_1/j\omega + c_1)m_2}{(k_1/j\omega + c_1 + j\omega m_2)} = m_1 + \frac{m_2\left[\omega_0^2 + j\omega(c_1/m_2)\right]}{(\omega_0^2 - \omega^2) + j\omega(c_1/m_2)}, \tag{4}$$

where $\omega_0 = \sqrt{k_1/m_2}$.

For $\omega \to 0$ relation $\mathbf{M}_x(0) = m_1 + m_2$ follows; which can be used for estimation of the value of mass m_2 at some stipulated low frequency, say, 0.75 Hz (4.712 rad/s).

In furthering this approach a rather good agreement between the measured apparent mass and the modelled apparent mass has been reached. However, a reasonable agreement in acceleration transmissibility across enabled horizontal (x-axis) VIS could not be obtained. Hence, the model would not be suitable for VIS performance predictions and so this approach was abandoned and will not be further treated.

4.3. A multibody model

Considering the steering wheel reaction in an analogy to the standard ISO 5982:2001 [11] the model according to Fig. 4(a) would be feasible. If a fore-and-aft (x-direction) VIS would be mounted to the seat and enabled (not blocked) the scheme would correspond to Fig. 4(b). Both pictures represent the same human body model, however in Fig. 4(b) horizontal (x-direction) VIS is included, so that the vibration transmissibility across this VIS can be measured and calculated. No direct resemblance to human body segments is anticipated. Following variables are used:

m_1… equivalent mass, corresponding to the seat armchair frame and cushions,
m_2… equivalent mass, corresponding to the sitting mass of the body,
m_3… equivalent mass accounting for the mass of a stipulated head,
k_1, c_1… equivalent stiffness and damping coefficient of the human body in the x-direction,
k_2, c_2 … equivalent stiffness and damping coefficient catering for the reaction of the human body to the steering wheel, exerted by hands (this may be in principle also an active force),
k_3, c_3… equivalent stiffness and damping coefficient due to the movement of the mass m_3,
k_0, c_0… stiffness and damping coefficient of the fore-and-aft suspension system of the seat, if enabled. Note that no dry-friction influence is assumed.

The dynamic variables are:

x_b… displacement of the simulator platform in the x-direction,
x_1… displacement of the seat frame in the x-direction; if the horizontal suspension system is disabled (blocked) $x_1 \equiv x_b$. If not, then the acceleration transmissibility T_x, corresponding

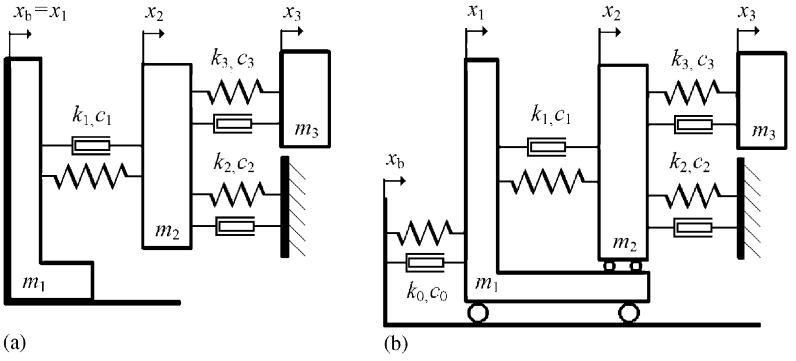

Fig. 4. Human body model in a cushioned suspended armchair part of a driver's seat with a fore-and-aft (x-direction) vibration isolating system: (a) horizontal VIS blocked; (b) horizontal VIS enabled.

to the rms ratio $\ddot{x}_1/\ddot{x}_b$ describes the x-direction vibration mitigation by the horizontal seat suspension,

x_2, x_3… displacements of the different model masses, not available to measurement.

The formula for apparent mass $\mathbf{M}_a$ for this multibody model is derived in following way:

(A) In the time domain the apparent mass $\mathbf{M}_a$ acting onto the horizontal VIS is given as: $M_a(t) = F(t)/\ddot{x}_1(t)$, where $F(t)$ is the acting force on mass m_1. The force $F(t)$ is given as:

$$F(t) = m_1\ddot{x}_1 + m_2\ddot{x}_2 + m_3\ddot{x}_3 + k_2x_2 + c_2\dot{x}_2. \tag{5}$$

(B) The complex apparent mass $\mathbf{M}_a(\omega)$ is then described as:

$$\mathbf{M}_a(\omega) = \frac{\mathbf{F}(\omega)}{\mathbf{a}(\omega)} = m_1 + \left[m_2 + \frac{c_2}{(j\omega)} + \frac{k_2}{(j\omega)^2}\right]\mathbf{H}_{21}(j\omega) + m_3\mathbf{H}_{31}(j\omega). \tag{6}$$

The respective transfer functions $\mathbf{H}_{21}(j\omega)$ and $\mathbf{H}_{31}(j\omega)$ are given by following formulas:

$$\mathbf{H}_{21}(j\omega) = \frac{\mathbf{X}_2(j\omega)}{\mathbf{X}_1(j\omega)} = \frac{m_3c_1(j\omega)^3 + (m_3k_1 + c_1c_3)(j\omega)^2 + (c_1k_3 + c_3k_1)(j\omega) + k_1k_3}{\mathbf{D}(j\omega)}, \tag{7}$$

$$\mathbf{H}_{31}(j\omega) = \frac{\mathbf{X}_3(j\omega)}{\mathbf{X}_1(j\omega)} = \frac{c_1c_3(j\omega)^2 + (c_1k_3 + c_3k_1)(j\omega) + k_1k_3}{\mathbf{D}(j\omega)}, \tag{8}$$

where the denominator $\mathbf{D}(\mathrm{j}\omega)$ is given as

$$\begin{aligned}\mathbf{D}(j\omega) = {} & m_2m_3(j\omega)^4 + [m_2c_3 + m_3(c_1 + c_2 + c_3)](j\omega)^3 + [m_2k_3 + m_3(k_1 + k_2 + k_3) \\ & + c_3(c_1 + c_2)](j\omega)^2 + [(c_1 + c_2)k_3 + c_3(k_1 + k_2)](j\omega) + k_3(k_1 + k_2).\end{aligned} \tag{9}$$

Note, that the formula for the apparent mass $\mathbf{M}_a(\omega)$ does not contain parameters k_0, c_0, i.e. the expression for apparent mass is independent of the seat horizontal VIS, as expected.

5. Models analysis

5.1. Introduction

The laboratory measurements with a single subject were undertaken at project partner's laboratory and passed on for analysis. The subject was sitting upright without seat belt in the "armchair" part of a selected driver's seat, equipped with a horizontal (x-axis) VIS, while the vertical VIS was removed. His feet were positioned on a footrest subjected to the same horizontal movement as the seat. The distance d between the seat and mock-up steering wheel was varied. Sets of data were made available under wide-band white noise excitation in the x-axis direction only in the frequency range 0.0–20.0 Hz with rms acceleration value $a_x = 0.40$ and $1.20\,\mathrm{m/s^2}$:

(i) Data from measurement of apparent mass in the fore-and-aft direction in respect to variation in distance d the fore-and-aft VIS blocked, as well as enabled.
(ii) Data from measurement of acceleration transmission T_x for two selected distances d, fore-and-aft VIS enabled.

No reliable phase information was supplied. Hence, a minimal phase system was assumed and only the measured apparent mass modules were further processed. Three variants of the above-introduced model of

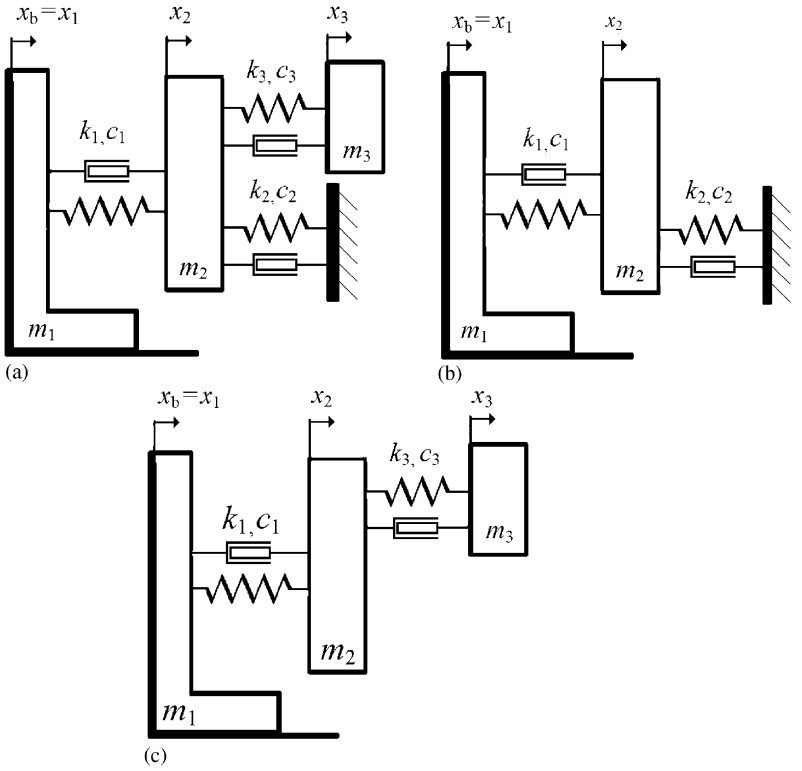

Fig. 5. Three model variants, used for detailed analysis: (a) variant "A"; (b) variant "B"; (c) variant "C".

Fig. 4, further denoted as "A", "B", "C", are possible (see Fig. 5):

(A) To analyse the full model as it stands—variant "A" (Fig. 5(a)).
(B) To assume a predominance of the steering wheel reaction leading to the possibility of neglecting the stipulated head movement, i.e. reducing the number of dof by forcing $m_3 = 0$, $k_3 = 0$, $c_3 = 0$, as depicted in Fig. 5(b)—variant "B".
(C) To assume a predominance of the stipulated head movement leading to the possibility to neglect the steering–wheel reaction. This also allows to reduce number of parameters by forcing $k_2 = 0$ and $c_2 = 0$ and corresponds to Fig. 5(c)—variant "C".

The ultimate test of applicability of one of the above approaches is the comparison of the simulated acceleration transmissibility T_x across the enabled horizontal suspension to that one measured in laboratory conditions.

In addition a measurement where the test subject had his HIL position, same as reported in Ref. [6], will be analysed too, assuming no steering wheel reaction.

5.2. Optimisation function

The measured data on apparent mass or frequency response function (FRF) courses are supposed to be supplied as N equidistantly sampled data points. A linear model is proposed, whose number of unknown parameters has to be less than N. The usage of the standard least-squares method and minimising the objective function, subject to some physically relevant constraints, facilitates the goodness of fit.

The objective function to be minimised is the sum of squares of differences of simulated M_{asim} apparent mass vs. measured M_{ameas} apparent mass modules. The quadratic error variable QE is then

evaluated as

$$\mathrm{QE} = \frac{1}{N}\sum_{i=1}^{N}\left(M_{\mathrm{asim}_i} - M_{\mathrm{ameas}_i}\right)^2, \tag{10}$$

where $i = 1, 2, \ldots, N$, is the number of evaluated points, i.e. values at different frequencies f_i. Further a relative error measure, $\mathrm{RE}_{\mathrm{avg}}$, has been calculated, defined as

$$\mathrm{RE}_{\mathrm{avg}} = \frac{1}{N}\sum_{i=1}^{N}\left|\frac{M_{\mathrm{ameas}_i} - M_{\mathrm{asim}_i}}{M_{\mathrm{asim}_i}}\right|. \tag{11}$$

The *MATLAB*® environment provides function *fminsearch* for this purpose. This is a multidimensional unconstrained nonlinear objective function minimisation programme code, using Nelder and Mead simplex algorithm [15]. However, for proper using of this function some a-priori knowledge of the model parameters vector has to be furnished. Being general in the nature the minimisation may lead to physically unacceptable values (e.g. negative masses); hence, a constrained optimisation had to be developed, limiting the search to a parameters subspace representing physically meaningful values. The damping is allowed to be negative, indicating active influence. To include these additional constraints the method of the so-called barrier function has been used, which enables to dynamically modify the step size during the search for the minimum of the objective function.

6. Results of measured apparent mass data identification

First the results of four apparent mass measurements at distances d of 200 and 250 mm have been analysed for the blocked suspension system. After a thorough analysis the mass m_1 value was fixed at a pre-set value of $m_1 = 5$ kg. Identification results for the three cases described in Fig. 5 are given in Table 1. Inspection of the last two columns can help to assess the "goodness of identification". This inspection reveals that there is virtually no difference in the variable QE value between the various variants; hence no clear indication of preference of any of the three variants, depicted in Fig. 5, can be given. The case "B" row 250GF1 (corresponding to Fig. 5(b)) is probably erroneous (a rather large value of QE) and leading to an sdof approach, excluded beforehand.

The same type of measurements has been performed for enabled horizontal VIS, complemented by measurement of acceleration transmissibility across the horizontal VIS. The apparent mass identification results for the three variants of Fig. 5 are condensed in Table 2. By inspection of the two last columns it can be

Table 1
Horizontal VIS blocked

	m_1 (kg)	m_2 (kg)	m_3 (kg)	k_1 (N/m)	c_1 (N s/m)	k_2 (N/m)	c_2 (N s/m)	k_3 (N/m)	c_3 (N s/m)	QE (kg^2)	$\mathrm{RE}_{\mathrm{avg}}$ (%)
(A)											
200GF1	5.0	59.5	1.4	39,347.0	702.2	158.0	90.1	971.0	12.1	6.905	2.99
200GF2	5.0	63.6	0.9	48,481.3	688.7	876.0	266.8	644.0	6.5	4.951	2.36
250GF1	5.0	56.2	0.9	29,091.8	412.9	521.2	222.8	676.3	4.4	8.040	4.67
250GF2	5.0	59.4	0.5	36,319.0	649.0	247.0	106.0	364.0	3.0	4.804	2.95
(B)											
200GF1	5.0	61.1	—	36,726.5	837.6	126.5	0.0	—	—	9.656	3.21
200GF2	5.0	61.0	—	43,431.0	932.6	118.6	0.0	—	—	7.676	3.09
250GF1	5.0	52.3	—	25,436.0	548.7	0.0	0.0	—	—	11.01	4.92
250GF2	5.0	58.3	—	34,059.9	731.5	112.1	0.0	—	—	5.649	3.11
(C)											
200GF1	5.0	57.6	1.3	37,631.2	749.7	—	—	864.4	11.0	7.134	3.08
200GF2	5.0	58.1	0.8	43,692.7	827.3	—	—	578.5	6.3	5.700	2.79
250GF1	5.0	51.9	1.0	25,178.0	506.4	—	—	224.8	5.1	7.684	4.37
250GF2	5.0	56.7	0.4	34,303.8	699.9	—	—	278.5	2.1	5.392	3.12

Table 2
Horizontal system enabled (loose)

	m_1 (kg)	m_2 (kg)	m_3 (kg)	k_1 (N/m)	c_1 (N s/m)	k_2 (N/m)	c_2 (N s/m)	k_3 (N/m)	c_3 (N s/m)	QE (kg^2)	RE_{avg} (%)
(A)											
200GF1	5.0	65.3	1.6	54,203.8	640.4	1708.0	283.7	1228.5	9.4	7.975	2.96
200GF2	5.0	58.6	4.8	47,793.1	390.5	1348.9	269.2	3876.5	66.9	11.08	3.09
250GF1	5.0	60.5	0.7	37,941.3	582.6	795.4	197.9	554.1	1.6	12.13	3.74
250GF2	5.0	65.0	1.1	46,480.2	645.7	1621.1	283.5	868.4	6.5	6.08	2.66
(B)											
200GF1	5.0	72.3	—	54,278.0	870.0	2166.7	287.7	—	—	23.31	4.37
200GF2	5.0	71.3	—	46,672.5	641.7	2054.4	284.7	—	—	22.97	4.83
250GF1	5.0	66.7	—	38,597.7	594.1	1631.8	279.6	—	—	19.57	4.65
250GF2	5.0	69.2	—	45,854.4	754.3	1841.4	285.1	—	—	12.87	3.68
(C)											
200GF1	5.0	32.1	18.4	47,112.5	17.7	—	—	12,248.4	461.8	10.85	2.85
200GF2	5.0	29.7	21.1	43,213.6	0.0	—	—	14,038.9	561.2	12.29	3.17
250GF1	5.0	18.7	31.4	44,814.3	0.0	—	—	20,421.0	927.8	15.86	3.59
250GF2	5.0	27.2	22.7	42,907.5	0.0	—	—	13,374.6	621.5	7.57	2.69

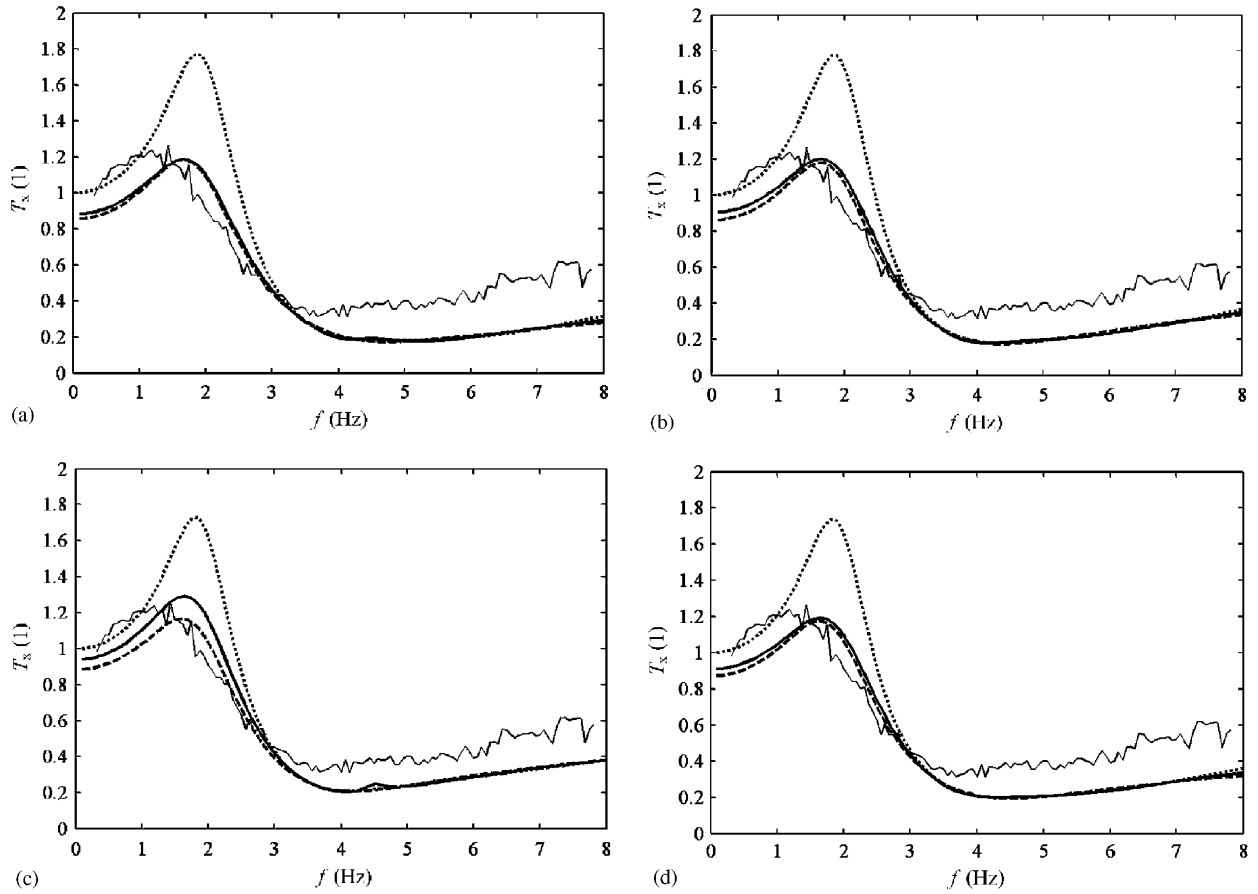

Fig. 6. Comparison of measured and simulated acceleration transmissibility through the horizontal VIS for three different apparent mass model variants: (a) measurement 200GF1; (b) measurement 200GF2; (c) measurement 250GF1; (d) measurement 250GF1; (measured (——); Model "A" (▬); Model "B" (▬ ▬ ▬); Model "C" (● ● ●)).

Table 3
Apparent mass—comparison of identified apparent mass model "A" parameters

H-VIS		m_1 (kg)	m_2 (kg)	m_3 (kg)	k_1 (N/m)	c_1 (N s/m)	k_2 (N/m)	c_2 (N s/m)	k_3 (N/m)	c_3 (N s/m)	QE (kg^2)	RE_{avg} (%)
Blocked	200GF1	5.0	59.5	1.4	39,347.0	702.2	158.0	90.1	971.0	12.1	6.905	2.99
	200GF2	5.0	63.6	0.9	48,481.3	688.7	876.0	266.8	644.0	6.5	4.951	2.36
	250GF1	5.0	56.2	0.9	29,091.8	412.9	521.2	222.8	676.3	4.4	8.040	4.67
	250GF2	5.0	59.4	0.5	36,319.0	649.0	247.0	106.0	364.0	3.0	4.804	2.95
Enabled	200GF1	5.0	65.3	1.6	54,203.8	640.4	1708.0	283.7	1228.5	9.4	7.975	2.96
	200GF2	5.0	58.6	4.8	47,793.1	390.5	1348.9	269.2	3876.5	66.9	11.08	3.09
	250GF1	5.0	60.5	0.7	37,941.3	582.6	795.4	197.9	554.1	1.6	12.13	3.74
	250GF2	5.0	65.0	1.1	46,480.2	645.7	1621.1	283.5	868.4	6.5	6.08	2.66

inferred, that the approach "B", i.e. neglecting the mass m_3 leads to unacceptable large errors in apparent mass estimation and has to be discarded. Tabulated results do not indicate any differences between approaches "A" and "C".

Moreover, the measured acceleration transmissibility across the enabled horizontal VIS has to be compared with the calculated transmissibility by each of the suggested models exposed to the same horizontal excitation acceleration (white noise in the frequency band range 0.0–20.0 Hz with rms acceleration value $a_x = 1.20\,\mathrm{m/s^2}$). The simulated transmissibility was calculated using the model depicted in Fig. 4(b), using parameters $k_0 = 12.0\,\mathrm{kN/m}$ and $c_0 = 600\,\mathrm{Ns/m}$, as supplied by the seat manufacturer. The seat exhibited a rather low dry-friction; hence, its influence could be neglected. The comparison in graphical form is depicted in Fig. 6 for all four measurements.

Fig. 6 indicates the match between the simulated and measured acceleration transmissibility and clearly disqualifies the variant "C", which does not account for the steering wheel reaction. There is no much difference between the variants "A" and "B", however in view of above conclusion the variant "A" is the most suitable one. Note the difference between the measured and simulated acceleration curve (a shift in the damped natural frequency in the acceleration transmissibility curves by some 0.5 Hz, as also noted in Ref. [9]). This phenomenon cannot be fully explained within the given set of measurements.

It is also interesting to compare the apparent mass values identified when the horizontal VIS was blocked or enabled. For the variant "A" the data are condensed in Table 3. Note there is no pronounced tendency in the parameters except the principal stiffness k_1, which increases by some 23% on the average (from 37.75 to 46.60 kN/m) and in the value of stiffness k_3 for the activated horizontal VIS (which exhibit distance d dependant decrease). The changes in the averaged masses m_2, m_3 due to activation of the horizontal VIS are not pronounced (the average m_2 value changes from 59.4 to 62.3 kg, whereas averaged value m_3 changes from 0.85 to 2.05 kg). Hence, it can be inferred that the model masses m_1, m_2, m_3 can be assumed as somehow fixed and only other parameters are being changed in respect to subject or posture variations.

7. Results of apparent mass measurements for hands in lap position

Using the same approach as above, data for Hands-In-Lap position were analysed too. Data supplied by project partner were used, as well values read of the apparent mass curve for this position as published by Fairley and Griffin in Ref. [6]. These data were obtained for the standard biodynamic position on a rigid seat, whereas the partner's data were obtained for a cushioned seat [9]. Firstly, all identification parameters were unconstrained. Results are depicted in Table 4 in sub-table denoted I. Note the rather good fit of the model with the experimental data—both the QE variable and the RE_{avg} variable is of an order of magnitude lower than in any of the previous cases. Two other approaches are further illustrated:

(i) reduction of the model to an sdof oscillatory system (Table 4, sub-Table II),
(ii) using a fixed pre-set value of $m_1 = 5\,\mathrm{kg}$ for the identification process (Table 4, sub-Table III).

Table 4
Apparent mass—hands in lap

	m_1 (kg)	m_2 (kg)	m_3 (kg)	k_1 (N/m)	c_1 (N s/m)	k_3 (N/m)	c_3 (N s/m)	QE (kg^2)	RE_{avg} (%)
(I)									
Fleury [8]	7.3	41.6	4.0	18,390.0	393.0	1161.0	46.0	0.203	1.08
Fairley [6]	9.4	38.7	18.7	53,144.0	733.0	6507.0	482.0	0.240	0.58
(II)									
Fleury [8]	6.3	47.3	—	17,064.0	536.0	—	—	6.347	6.84
Fairley [6]	10.2	57.0	—	37,931.0	1296.0	—	—	9.442	5.06
(III)									
Fleury [8]	5.0	41.9	4.9	18,492.0	384.0	1324.0	62.0	0.343	1.16
Fairley [6]	5.0	36.5	24.4	55,674.0	665.0	7393.0	663.0	0.326	0.68

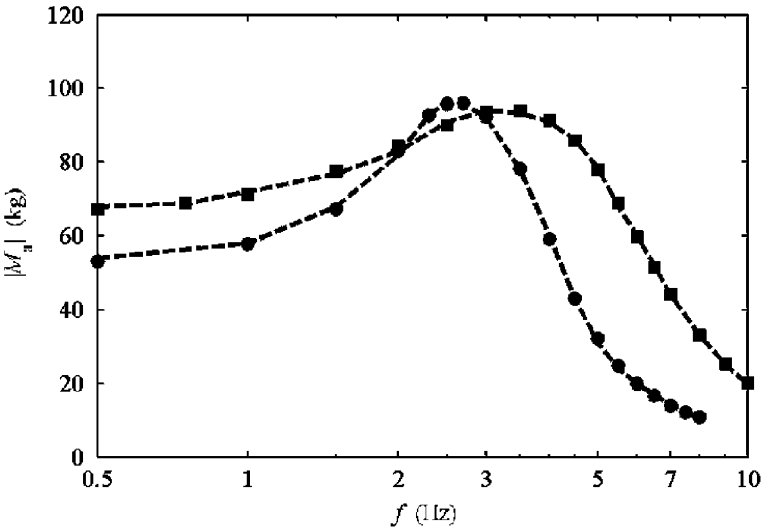

Fig. 7. Courses of identified apparent masses (▬ ▬ ▬) for fixed $m_1 = 5$ kg, compared to measured data (●—Fleury's data, ■—Fairley's data).

By inspection of sub-Table II it is clearly seen, that this model reduction is not applicable, since the QE value is rather large. Using a fixed m_1 value does not markedly deteriorate the identification—the QE value of sub-Table III did not substantially change in respect to the value of sub-Table I. Thus, this approach is justified. The good match between the measured values and the identified apparent mass curves is also illustrated in Fig. 7. The differences in the curves maxima can be attributed to different experimental conditions and possibly to different test subject masses.

8. Results of apparent mass dependence on the distance *d*

In Fig. 2, apparent mass moduli plots in dependence on a distance d are depicted. It is interesting to apply the developed model structure to these data and assess the dependence of various model parameters on this distance. Two variants "A" and "B" were analysed. The data were processed in the same way as described and the results are condensed in Tables 5 and 6 and depicted in graphical form in Figs. 8 and 9. Additionally, the damped natural frequencies f_{2d} and f_{3d} and damping ratios ξ_2 and ξ_3, corresponding to model masses m_2 and

Table 5
Model variant "A"—the dependence of identified parameters on the distance d

d (mm)	m_1 (kg)	m_2 (kg)	m_3 (kg)	k_1 (N/m)	c_1 (N s/m)	k_2 (N/m)	c_2 (N s/m)	k_3 (N/m)	c_3 (N s/m)	f_{2d} (Hz)	ξ_2 (1)	f_{3d} (Hz)	ξ_3 (1)	QE (kg^2)	RE_{avg} (%)
100/150	5	65.3	2.3	38,817	355.1	429.5	198	1128.8	24.6	3.894	0.178	3.422	0.241	2.92	3.11
200/250	5	63.7	1.3	37,430	703.1	463.9	147.8	3,030.9	1.1	3.891	0.264	7.685	0.009	6.04	2.31
300	5	55.1	1.0	26,121	428.9	538.4	171.9	1068.5	5.8	3.461	0.245	5.182	0.089	1.63	1.88
HIL	5	44.9	3.3	18,795	403.8	29.4	47.3	934	33.6	3.226	0.257	2.552	0.303	0.36	1.55

Table 6
Model variant "B"—the dependence of identified parameters on the distance d

d (mm)	m_1 (kg)	m_2 (kg)	k_1 (N/m)	c_1 (N s/m)	k_2 (N/m)	c_2 (N s/m)	f_{2d} (Hz)	ξ_2 (1)	QE (kg^2)	RE_{avg} (%)
100/150	5	72.2	40,089	511.0	689.0	220.8	3.695	0.213	7.83	3.24
200/250	5	64.5	36,897	676.9	471.7	148.3	3.693	0.266	7.73	3.62
300	5	55.7	25,581	414.5	485.9	166.5	3.341	0.241	1.99	2.32
HIL	5	54	19,473	489.2	422.1	164.8	2.899	0.315	3.57	4.58

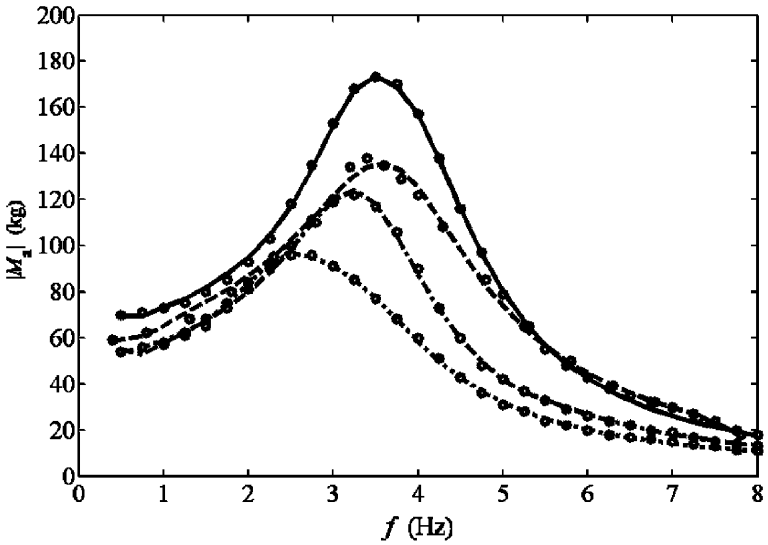

Fig. 8. Model "A"—measured vs. simulated apparent mass: $d = 100/150$ mm (▬); $d = 200/250$ mm (▬ ▬ ▬); $d = 300$ mm (▬ ● ▬); HIL (●●●); measured values (O O O).

m_3, respectively, were calculated and are given in the tables. By inspection of both tables it can be seen that the variant "A" fits the measured values better than the model "B"—the error indicators QE and RE_{avg} are less for variant "A" than for the variant "B".

9. Discussion

Owing to a rather limited amount of data available obtained with a single test subject only obviously no statistical analysis is possible. Such a research has to be undertaken at another occasion, having at hand a cohort of suitable test persons, which was not the case here. However the discussion, with some caution,

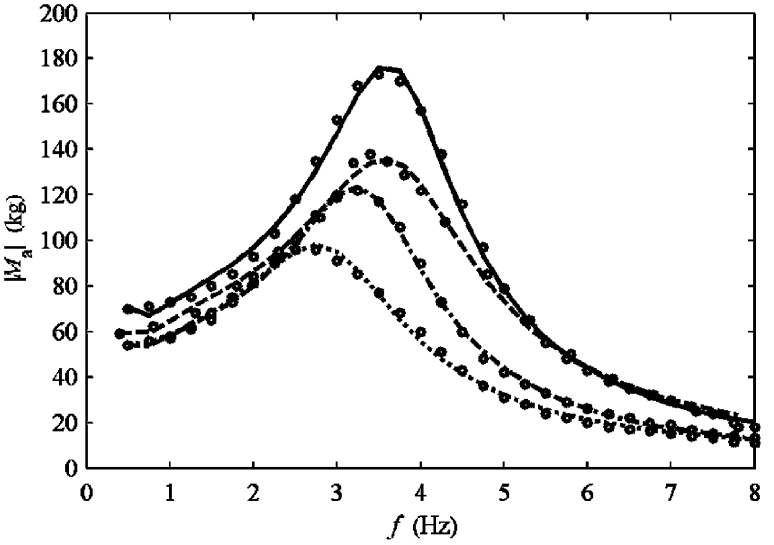

Fig. 9. Model "B"—measured vs. simulated apparent mass: $d = 100/150$ mm (▬); $d = 200/250$ mm (▬ ▬ ▬); $d = 300$ mm (▬ ● ▬); HIL (● ● ●); measured values (O O O).

can be focused on following issues:

(i) Does the proposed model reasonably fit the available experimental data, i.e. is the model a good descriptor of the x-direction apparent mass of a human body sitting in an upright position in a cushioned "armchair" part of commercial driver's seat?
(ii) Can be the proposed model reasonably used for x-direction vibration transmissibility prediction of a fore-and-aft (x-axis) horizontal suspension?
(iii) Can the proposed model explain to certain extent the dependence of the measured apparent mass on the distance d between the seated driver and the steering wheel, as manifested in Fig. 2?

In authors view, a cautious answer to the two above-mentioned points, subjected to limitation posed by the rather limited amount data available hitherto, is given by Fig. 6. The model variant "A" of Fig. 5(a) enables to describe the measured apparent mass data and with some caution the prediction of vibration transmissibility across the x-direction horizontal VIS. Hence, it could be used in principle for the horizontal seat suspension modelling and optimisation, which were one of the aims of the VIBSEAT Project. Obviously, the model is far from being flawless and thoroughly validated. In analogy with the standard ISO 5982:2001 [11], extensively used for modelling human body behaviour in the vertical direction, it is a rather simple one, without much resemblance to human body segments. However, it includes the main features—a sitting mass, a steering wheel interaction and another oscillatory dof. The analysis indicated, that these model components are indispensable—reducing the model from variant "A" to either variant "B" or "C" (see Fig. 5) leads either to worsening of fit to experimentally determined values of apparent mass or to model inability to predict the vibration transmissibility. This was also the substantial drawback of a simpler sdof model, depicted in Fig. 3. At the present level of knowledge there are no ways to decompose this model into the human body part and into the seat back-support cushioning part. This requires further measurements and their analysis.

Another factor has to be pointed out—models sensitivity to the steering wheel reaction, described by parameters k_2, c_2 and their values. From inspection of Table 3 six cases, in which the value of c_2 is around 260 N s/m, can be identified. These curves correspond well with those measured, essentially as depicted in Fig. 6 for case "A". However, for the two other values the simulated acceleration transmissibility course approaches the curve of case "B", rather than that one of variant "A". Hence, the exact value of equivalent damping c_2 markedly determines the match between simulated and measured acceleration transmissibility. As in practical situations parameters k_2, c_2 are probably dependant on driver's conscious or sub-conscious

homoeostatic reactions, it may be somehow difficult to obtain a reproducible set of parameters for all the various situations occurring in practical life, as indicated in Chapter 3. However, the limited number of measurements made with one test subject only is not sufficient for a more detailed discussion.

The assessment of the influence of the distance d between the seated driver and the steering wheel can be best illustrated by the tabulated results of variant "B". These are somehow simpler to interpret as variant "A" (Fig. 5), although the tendency is the same:

(i) If the values for $d = 100$–150 mm are compared to those for $d = 200$–250 mm from Table 6 it can be inferred, that the damped natural frequency f_{d2} is virtually the same, but the damping ratio ξ_2 changes, as also readily seen from Fig. 9.
(ii) If the values for the three distances d are compared with each other and with the HIL value there is a slight discrepancy. A tendency is still visible—the damped natural frequency f_{d2} decreases with increasing distance d and the damping ratio ξ_2 increases.
(iii) There is a marked difference in the stiffness k_1 value—for the distances $d = 100$–150 and 200–250 mm the value of k_1 is high—40 and 36.9 kN/m, respectively; whereas for the distance $d = 300$ mm and for the HIL position the value of k_1 is low—25.6 and 19.5 kN/m, respectively. Hence, the value of stiffness k_1 seems to be a good distinctive factor on the distance between the seated driver and the steering wheel.

There is virtually no difference in the apparent mass curves in Figs. 8 and 9. From the limited amount of available data it is very difficult to stipulate a functional dependency of the apparent mass parameters on the distance d (except of the above observation), despite of resemblance of the apparent mass curves to the curve of the FRF modulus of an sdof oscillatory system with variable damping, as originally assumed and Fig. 2 would suggest.

10. Preliminary conclusions

From the analysed apparent mass measurements with a single subject in laboratory environment following preliminary conclusions can be cautiously drawn:

(1) The measured apparent mass data in the x-direction can be modelled using standard translatory mechano-mathematical "building blocks"—masses m_i, stiffnesses k_j and linear viscous damping coefficients c_i, in an analogy to similar approach for the vertical direction (z-axis) as introduced by the respective ISO and DIN standards [11,12].
(2) A simple single dof model is not suitable, as it does not account for all the phenomena. It seems, that the suggested model (termed variant "A" of Fig. 5(a)) sufficiently describes the seated human body behaviour in the frequency range 0.5 Hz to some 7.0 Hz.
(3) The steering wheel reaction has to be taken into account for many real-life positions of driver's sitting upright or slightly inclined backward in a cushioned suspended "armchair" type driver's seat. The steering wheel reaction is dependant on many factors, especially on the distance between the seated driver and the steering wheel, on to the extent of back contact with the back support and use of seat belts, as well as on driver's homoeostatic behaviour.
(4) The extent of steering wheel reaction (described in the most simple way by a linear stiffness and a linear viscous damping) is crucial for evaluation of acceleration transmissibility through a fore-and-aft (x-direction) seat suspension system, if mounted and enabled.
(5) It might be difficult to reproduce in laboratory all practical driving conditions with sufficient accuracy. Hence the apparent mass model parameters, as established from identification of laboratory measurements in well-defined conditions may not be fully applicable for modelling of x-direction vibration influence on a seated driver in all practical driving conditions.
(6) The hands-in-lap position yields a far better match between the apparent mass model parameters and the measured apparent mass data than the hands-on wheel positions; the QE and RE_{avg} measures are substantially lower (see respective entries in Tables 3 and 4). It is independent of the steering wheel reaction and hence would allow a more reproducible assessment of vibration influence on seated human body in the x-direction.

The proposed model, based on a rather limited amount of available information, could become a starting point for further measurements, analysis and discussion. The model is proposed for further use in biodynamical research and for research of cushioned seats equipped with fore-and-aft VIS as one possible approach to modelling of this rather complex problem. The model has to be validated with a cohort of test subjects. Furthermore, there is still much space in experiment design and parameters variation, which could not have been obviously handled by one laboratory with limited resources and available number test subjects within reasonable time.

Acknowledgements

This research was conducted within the VIBSEAT project, funded by the European Commission FP5 "Growth" programme, co-coordinated by the Human Factors Research Unit, ISVR, University of Southampton, UK (Contract no. G3RD-CT-2002-00827). The support of the Commission is fully acknowledged. The analysed data were made available by one of the VIBSEAT Project partner—the *Institut National de Recherche et de Sécurité* of Nancy, France.

References

[1] M.J. Griffin, *Handbook of Human Vibration*, Academic Press, London, 1990.
[2] D.V. Balandin, N.N. Bolotnik, W.D. Pilkey, *Optimal Protection from Impact, Shock and Vibration*, Gordon and Breach Science Publishers, Amsterdam, 2001.
[3] N.J. Mansfield, *Human Response to Vibration*, CRC Press, Boca Raton, 2005.
[4] M.J. Griffin (Ed.), Special issue on WBV injury conference, *Journal of Sound and Vibration* 215 (4) (1998) 593–996.
[5] M.J. Griffin (Ed.), Special issue on WBV injury conference, *Journal of Sound and Vibration* 253 (1) (2002) 1–327.
[6] T.E. Fairley, M.J. Griffin, The apparent mass of the seated human body in the fore-and-aft and lateral directions, *Journal of Sound and Vibration* 139 (2) (1990) 299–306.
[7] P. Holmlund, R. Lundström, Mechanical impedance of the human body in the horizontal direction, *Journal of Sound and Vibration* 215 (1998) 801–812.
[8] N.J. Mansfield, R. Lundström, The apparent mass of the human body exposed to non-orthogonal horizontal vibration, *Journal of Biomechanics* 32 (1999) 1269–1278.
[9] G. Fleury, Experimentelle Untersuchung der dynamischer Masse einer sitzender Versuchsperson bei Schwingungen in der X-Richtung zur Bildung eines Modells, Tagung "Humanschwingungen" Darmstadt, *VDI Berichte* 1821 (2004) 301–316.
[10] G. Fleury, P. Mistrot, A model to predict the dynamical behaviour of a seated subject exposed to fore-and-aft vibrations, *Proceedings of the WBV Injury 2005 Conference*, Nancy, France, June 2005.
[11] International Organization for Standardization ISO 5982, Mechanical vibration and shock—range of idealized values to characterize seated-body biodynamic response under vertical vibration, 2001.
[12] Deutsches Institut für Normung E. v. DIN 45676, Driving point Mechanical Impedance and Transfer Functions of the Human Body, 2003 (in German).
[13] N. Nawayaseh, Modelling the vertical and fore-and-aft forces caused by whole-body vertical vibration, *Proceedings of the 37th United Kingdom Conference on Human Responses to Vibration*, Department of Human Sciences, Loughborough University, Leicestershire, UK, 2002 (pp. 302–320).
[14] S. Nishiyama, N. Uesugi, T. Takeshima, Y. Kano, H. Togii, Research on vibration characteristics between human body and seat, steering wheel and pedals (effects of seat position on ride comfort), *Journal of Sound and Vibration* 236 (1) (2000) 1–21.
[15] Matlab, *Using Matlab, Version 6*, The MathWorks, Inc., Natick, MA, 1984–2000.